ANTIMICROBIAL AGENTS AND CHEMOTHERAPY, Nov. 2005, p. 4437–4442 Vol. 49, No. 11
0066-4804/05/$08.00+0 doi:10.1128/AAC.49.11.4437–4442.2005

Application of Quantitative Real-Time Reverse Transcription-PCR in Assessing Drug Efficacy against the Intracellular Pathogen *Cryptosporidium parvum* In Vitro

Xiaomin Cai,[1] Keith M. Woods,[2] Steve J. Upton,[2] and Guan Zhu[1]*

Department of Veterinary Pathobiology, College of Veterinary Medicine, Texas A&M University, 4467 TAMU, College Station, Texas 77843,[1] and Division of Biology, Kansas State University, Manhattan, Kansas 66506[2]

Received 25 May 2005/Returned for modification 4 June 2005/Accepted 2 August 2005

We report here on a quantitative real-time reverse transcription-PCR (qRT-PCR) assay for assessing drug efficacy against the intracellular pathogen *Cryptosporidium parvum*. The qRT-PCR assay detects 18S rRNA transcripts from both parasites, that is, the cycle threshold for 18S rRNA from parasites ($C_{T[P18S]}$) and host cells ($C_{T[H18S]}$), and evaluates the relative expression between parasite and host rRNA levels (i.e., $\Delta C_T = C_{T[P18S]} - C_{T[H18S]}$) to minimize experimental and operational errors. The choice of qRT-PCR over quantitative PCR (qPCR) in this study is based on the observations that (i) the relationship between the logarithm of infected parasites (log[*P*]) and the normalized relative level of rRNA ($\Delta\Delta C_T$) is linear, with a fourfold dynamic range, by qRT-PCR but sigmoidal (nonlinear) by qPCR; and (ii) the level of RNA represents that of live parasites better than that of DNA, because the decay of RNA (99% in ~3 h) in dead parasites is faster than that of DNA (99% in ~24 to 48 h) under in vitro conditions. The reliability of the qRT-PCR method was validated by testing the efficacies of nitazoxanide and paromomycin on the development of two strains of *C. parvum* (IOWA and KSU-1) in HCT-8 cells in vitro. Both compounds displayed dose-dependent inhibitions. The observed MIC_{50} values for nitazoxanide and paromomycin were 0.30 to 0.45 μg/ml and 89.7 to 119.0 μg/ml, respectively, comparable to the values reported previously. Using the qRT-PCR assay, we have also observed that pyrazole could inhibit *C. parvum* development in vitro (MIC_{50} = 15.8 mM), suggesting that the recently discovered *Cryptosporidium* alcohol dehydrogenases may be explored as new drug targets.

Cryptosporidium parvum is an intracellular parasitic protist that infects both humans and animals (5, 22). This parasite belongs to the phylum Apicomplexa. However, recent phylogenetic reconstructions have suggested that the genus *Cryptosporidium* probably represents an early branch at the base of the phylum (31). Together with *C. hominis* (a new species recently renamed from type 1 *C. parvum*) (15), *C. parvum* is also a significant opportunistic pathogen among immunocompromised individuals (e.g., AIDS patients) (5). Currently, only a single drug (i.e., nitazoxanide [NTZ]) has been approved for the treatment of cryptosporidiosis in the United States and Central and South America (10; see also http://www.romark.com). Therefore, there is a need for the development of new anti-*Cryptosporidium* drugs.

In vitro drug testing is a critical step in the early stage of drug development. To evaluate drug effects against *C. parvum* in vitro, parasites must be cultured by infecting human or animal cells. Currently, several techniques are available for the evaluation of drug efficacy against *C. parvum* in vitro. These techniques include the microscopic method (by counting the number of fluorescently labeled or chemically stained parasites per microscopic field) (8), microtiter enzyme-linked immunosorbent assay (25, 26), chemiluminescence immunoassay (28, 29), and potentially real-time quantitative PCR (qPCR) (6, 13). While all methods may reliably detect the level of parasites in vitro, many have their own limitations. The microscopic method can be labor-intensive and highly subjective. Antibody-based techniques rely on the availability of good antibodies and are limited by the sensitive and limited signal-to-noise ratio (25). More recently, a real-time qPCR-based method has been introduced for assessment of the effects of drugs against *C. parvum* in vitro by detecting the level of parasite DNA, and this method promised a wide dynamic range of detection (6, 13). However, our recent observations suggest that the DNA level may not always be well correlated with the number of infected parasites because the relationship between the inoculated number of parasites and the normalized cycle thresholds (C_Ts) of detection by qPCR is not linear. Furthermore, the DNA from dead parasites may also exist in these samples (see below for details). In addition, the reported qPCR method displayed significant plate-to-plate variations (13), indicating that improvements are needed to take full advantage of the real-time PCR system for drug testing.

Here we report on an improved method for assessment of drug efficacy against *C. parvum* infection in vitro, based on the quantitative real-time reverse transcription-PCR (qRT-PCR) technique. By detecting the level of 18S rRNA from parasites, this method is more likely to detect only live parasites that survive during the drug treatment. The qRT-PCR method also includes the detection of host cell 18S rRNA as an internal control, and the parasite level is assessed by the ratio (relative expression) of parasite and host 18S rRNA levels. The reliability of the qRT-PCR assay was validated by assessing the efficacy of NTZ (the only approved anticryptosporidial medicine) and paromomycin (a well-established reference compound)

* Corresponding author. Mailing address: Department of Veterinary Pathobiology, College of Veterinary Medicine, Texas A&M University, 4467 TAMU, College Station, TX 77843. Phone: (979) 845-6981. Fax: (979) 845-9972. E-mail: gzhu@cvm.tamu.edu.

against two distinct strains (IOWA and KSU-1) of *C. parvum*. In addition, the newly established qRT-PCR method was also used to assess the in vitro efficacy of pyrazole, an alcohol dehydrogenase (ADH) inhibitor, against the growth of *C. parvum* in vitro.

MATERIALS AND METHODS

Parasite cultivation. Only *C. parvum* oocysts (IOWA and KSU-1 strains) less than 3 months old (since the time of harvest from infected calves) were used in all experiments. Oocysts were purified by Percoll gradient centrifugation and bleached briefly as described previously (16, 30). HCT-8 cells (2.5×10^5/well) were seeded in 24-well plates and allowed to grow overnight or until they reached ~80% confluence at 37°C with 5% CO_2 in RPMI 1640 medium containing 10% fetal bovine serum, 15 mM HEPES, and other supplements, as described previously (4, 23). For the generation of standard curves, host cells were infected with 10-fold serial dilutions of parasite oocysts, with host cell-to-parasite ratios ranging from 5:1 to 50,000:1 (i.e., 50,000 to 5 oocysts/well). For drug testing, host cells were infected with 50,000 oocysts per well. In all experiments, parasites were allowed to incubate at 3 h at 37°C for excystation and invasion into host cells. Parasites that failed to invade host cells were removed from the plates by an exchange of the culture medium. Negative controls that received no parasites were included in each experiment. To make stock solutions of compounds, paromomycin or pyrazole (both from Sigma-Aldrich Inc., St. Louis, MO) was dissolved in water, while NTZ (Sequoia Research Products Ltd., Oxford, United Kingdom) was dissolved in 1% dimethyl sulfoxide. All compounds were then added to the infected cells at the specified final concentrations during the medium exchange. Parasite-infected cells were then incubated at 37°C with 5% CO_2 for 44 h. At least two wells in different plates were employed for each experimental condition, and all experiments were repeated two or more times.

qRT-PCR and qPCR. Total RNA and genomic DNA (gDNA) were isolated from parasite-infected cells at 44 h postinfection by using RNeasy and DNeasy isolation kits (QIAGEN Inc., Valencia, CA), respectively. The concentrations and the quality of the RNA and the DNA in each sample were determined by measuring their absorbances at 260 and 280 nm, respectively. All RNA and gDNA samples were adjusted to a concentration of 20 ng/μl. The detection of parasite 18S rRNA employed a pair of previously published primers (i.e., primers Cp18S-995F [5′-TAG AGA TTG GAG GTT GTT CCT-3′] and Cp18S-1206R [5′-CTC CAC CAA CTA AGA ACG GCC-3′]) (1, 4). The primers specific to human 18S rRNA (primers Hs18S-F1373 [5′-CCG ATA ACG AAC GAG ACT CTG G-3′] and Hs18S-R1561 [5′-TAG GGT AGG CAC ACG CTG AGC C-3′]) were designed after comparison of published sequences of the human and *Cryptosporidium* 18S rRNA genes. The expected sizes of the amplicons obtained by using these two pairs of primers were 212 bp and 189 bp, respectively. A SYBR green-based real-time RT-PCR protocol was employed by using an iScript One-Step RT-PCR kit with SYBR green (Bio-Rad Laboratories, Hercules, CA). Reaction mixtures containing 20 ng total RNA; and appropriate amounts of reagents and primers were first incubated at 48°C for 30 min to synthesize cDNA, heated at 95°C for 15 min to inactivate the reverse transcriptase, and then subjected to 40 thermal cycles (95°C for 20 s, 50°C for 30 s, and 72°C for 30 s) of PCR amplification with an iCycler iQ real-time PCR detection system (Bio-Rad Laboratories). The qPCR analysis was performed similarly with 20 ng gDNA (IOWA strain only) as the template in each reaction, but reverse transcriptase and the reverse transcription step were omitted. At least two replicate reactions were performed for each sample.

Quantitative analysis by qRT-PCR. For each sample, the C_Ts for detection of the 18S rRNA levels of parasites ($C_{T[P18S]}$) and host cells ($C_{T[H18S]}$) were determined by qRT-PCR. The relative level of parasites in each sample was first determined by measurement of the ratio between those of parasite and host cells, i.e., the difference between $C_{T[P18S]}$ and $C_{T[H18S]}$ (ΔC_T):

$$\Delta C_T = C_{T[P18S]} - C_{T[H18S]} \quad (1)$$

Next, in each of experiments all ΔC_T values (relative levels of *C. parvum* 18S rRNA) were further normalized by subtracting from them the mean of the ΔC_T values derived from the samples infected with highest number of parasites (the set of lowest ΔC_T values). This resulted in the normalized relative levels of parasite 18S rRNA among different samples ($\Delta\Delta C_T$). For example, in a group of five samples (infected with 5 to 50,000 oocysts/well) each ΔC_T value (represented by ΔC_{Tn}, where $n = 1$ to 5) was reduced by the mean of the ΔC_T values derived from samples infected with 50,000 oocysts/well (represented by ΔC_{T1}), as indicated by

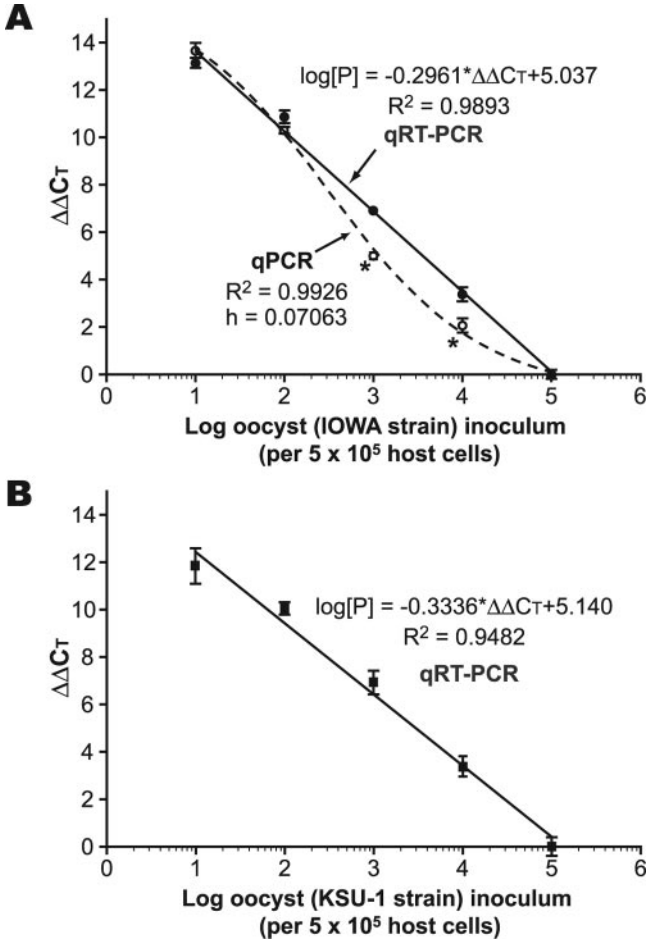

FIG. 1. Standard curves for IOWA strain (A) and KSU-1 strain (B) of *C. parvum* infection in HCT-8 cells as determined by qRT-PCR (solid line) and qPCR (dashed line) by detecting the parasite and host cell 18S rRNA and 18S rRNA gene. At each oocyst inoculum level, the mean $\Delta\Delta C_T$ values were derived from two sample replicates, and each sample was subjected to at least two qRT-PCRs or qPCRs. The qRT-PCR curve was derived by a linear regression between the $\Delta\Delta C_T$ values and the logarithm of oocyst inoculum (presented here as the number of oocysts per 10^6 host cells), whereas the qPCR curve was derived by a nonlinear regression by using a four-parameter logistic equation (see equation 9 in Materials and Methods). Bars represent standard errors of the means.

$$\Delta\Delta C_{Tn} = \Delta C_{Tn} - \Delta C_{T1} \quad (2)$$

For the calculation of standard curves, the $\Delta\Delta C_T$ values were plotted against the logarithm of the number of inoculated parasite oocysts (log[*P*]). After linear regression, the following relationship was obtained:

$$\log[P] = A \cdot \Delta\Delta C_T + B \quad (3)$$

where *A* is the slope of the regression line and *B* is the intersection and in one of our standard curves were found to be 0.2961 and 5.037, respectively (Fig. 1A). To evaluate the efficacies of NTZ, paromomycin, and pyrazole against *C. parvum*, the normalized relative levels of pathogen between experimental samples (P_{exp}) (with drug treatment) and controls (P_{ctl}) (without drug treatment) were determined for computation of the percent inhibition. For this purpose, we first determined the relationship between the logarithms of P_{exp} and P_{ctl}:

$$\log(P_{exp}/P_{ctl}) = \log P_{exp} - \log[P_{ctl}] = A \cdot (\Delta\Delta C_T - \Delta\Delta C_{T[ctl]}) \quad (4)$$

where *A* represents the slope of the regression line. The resulting equation (equation 4) indicates that the logarithm of the normalized relative level of

pathogen between two experimental samples is defined only by the slope (value *A*) and $\Delta\Delta C_T$. The intersection (value *B*) is not needed to calculate percent inhibition. Because all samples were normalized against uninfected controls, $\Delta\Delta C_{T[\mathrm{ctl}]}$ would equal zero and the previous equation (equation 4) could be simplified to

$$\log(P_{\mathrm{exp}}/P_{\mathrm{ctl}}) = A \cdot \Delta\Delta C_T \quad (5)$$

From equation 5, the relative level of parasites between experimental and control samples were calculated as follows:

$$P_{\mathrm{exp}}/P_{\mathrm{ctl}} = 10^{A \cdot \Delta\Delta C_T} \quad (6)$$

$$P_{\mathrm{exp}}/P_{\mathrm{ctl}} = \varepsilon^{-\Delta\Delta C_T} \quad (7)$$

The parameter ε is commonly referred to as the amplification efficiency, which should normally range between 1 (no amplification) and 2 (100% amplification efficiency) (24). However, one must distinguish the ε value from the "percent PCR efficiency" calculated directly by the programs implemented in some real-time PCR systems, which may actually equal $(\varepsilon - 1) \cdot 100$.

The inhibition curves derived from equation 6 or 7 were subject to nonlinear regression (curve fit) against log-transformed drug concentrations by using the Prism v4.0 program (GraphPad Software, San Diego, CA). The MIC_{50} for each compound was typically derived from the sigmoidal model by determining the drug concentrations that caused a 50% reduction of parasite growth in comparison to the growth of the controls. In addition, percent inhibition curves commonly used for the presentation of drug inhibition data could also be computed by using following equation:

$$\%\ \text{inhibition} = [1 - (P_{\mathrm{exp}}/P_{\mathrm{ctl}})] \cdot (100\%) = (1 - 10^{A \cdot \Delta\Delta C_T}) \cdot (100) \quad (8)$$

Nonlinear regression analysis and computation of the MIC_{50} may also be performed for the data sets derived by using equation 8 by using an appropriate curve-fitting model. For computation of standard errors (SEs), the mean of the normalized value in all control samples (i.e., $\Delta\Delta C_{T[\mathrm{ctl}]}$) was calculated first for each set of experiments (e.g., all data derived from the one plate) as a normalization baseline. The percent inhibition and SE values of all samples (including those of the controls) can then be calculated individually from the normalized $\Delta\Delta C_T$ values.

Quantitative analysis by qPCR. The qPCR analysis was performed only for samples infected with various numbers of the IOWA parasite strain. Similar to qRT-PCR analysis, the $\Delta\Delta C_T$ values were calculated for each set of experiments. However, we determined that for qPCR, the relationship between the $\Delta\Delta C_T$ values and the logarithm of infected parasites (i.e., oocyst numbers) was sigmoidal rather than linear. Therefore, only nonlinear regressions of qPCR data were performed to generate best-fit sigmoidal curves by using the Prism v4.0 program with the following four-parameter logistic equation:

$$Y = \text{bottom} + (\text{top} - \text{bottom})/(1 + 10^{(\log[\mathrm{EC}_{50}] - X) \cdot h}) \quad (9)$$

For the reasons discussed below, the qPCR method was not used for assessment of the efficacies of NTZ, paromomycin, or pyrazole against *C. parvum* growth in vitro.

Decay of RNA and DNA from dead *C. parvum* sporozoites. To test how long the RNA and DNA in dead parasites could exist in the current in vitro system, we prepared free sporozoites (IOWA strain) by excystation of fresh oocysts and inactivated them by three cycles of freezing (−80°C for 1 h) and thawing (room temperature for 30 min). HCT-8 cells were cultured in 24-well plates as described above. Dead sporozoites (200,000 per well) were added to the cultured HCT-8 cells by a medium change and incubated at 37°C for 1, 3, 6, 16, and 48 h. Each experimental condition included at least two replicates. At each specified time point, the supernatant in each well was collected and centrifuged, and the pellet was combined with its corresponding monolayer for the isolation of total RNA and gDNA for qRT-PCR and qPCR analyses. In both analyses, the $\Delta\Delta C_T$ values were calculated and the relative amount of detectable parasite 18S rRNA and 18S rRNA gene were computed according to their corresponding standard curves.

RESULTS

Comparison of qRT-PCR and qPCR assays. In this study, we chose to derive standard curves from samples infected with a serially diluted numbers of parasites rather than from serially diluted, purified RNA or DNA. Therefore, the relationship between $\Delta\Delta C_T$ and normalized levels of parasite 18S rRNA that were determined should truly reflect the level of parasites. The two sets of primers employed in this study were specific to their corresponding templates, as no detectable nonspecific products were observed by melting curve analysis or agarose gel electrophoresis of their amplicons (data not shown). We first tested the linearity of the data generated by qRT-PCR (IOWA and KSU-1 strains) and qPCR (IOWA strain) in samples infected with 5 to 50,000 oocysts (per ~250,000 HCT-8 cells). We observed that the relationships between normalized $\Delta\Delta C_T$ values and the parasite levels (in a wide range of 4 orders of magnitude) were highly linear in the qRT-PCR assay for both the IOWA and the KSU-1 strains (Fig. 1A and B) but were apparently nonlinear (sigmoidal) in the qPCR assay (Fig. 1A).

Although nonlinear regression could generate a well-fit sigmoidal curve for the qPCR data ($R^2 = 0.9926$) for calculation of the parasite level in experimental samples (IOWA strain) (Fig. 1A, dashed line), the computation would be more complicated than the use of the linear standard curve produced by qRT-PCR (Fig. 1A and B, solid lines). The mechanism behind the unexpected sigmoidal relationship between $\Delta\Delta C_T$ and the number of infected *C. parvum* oocysts in the qPCR assay was unclear. Similar nonlinearity in a qPCR assay was recently observed in a study where 5 to 250 oocysts were infected per well in 96-well microplates (i.e., ~2 orders of magnitude), although linearity was apparent among samples infected with 5, 25, and 50 oocysts (i.e., within 1 order of magnitude) (see Fig. 2 in reference 6). Since the qPCR assay detects the level of the 18S rRNA gene and since DNA replication is associated with the parasite cell cycle, we speculate that the rate of DNA replication in cultured *C. parvum* cells may vary slightly depending on the density of parasites (i.e., faster cell cycles in samples with host cell:oocyst inoculum ratios ranging from 50:1 to 500:1) (Fig. 1A, points marked with asterisks).

The advantage of using qRT-PCR to quantify the growth of *C. parvum* in vitro is further supported by the RNA and DNA decay data determined by qRT-PCR and qPCR, respectively (Fig. 2). In this experiment, ~99% of RNA in dead sporozoites (IOWA strain) decayed within 3 h under current cell culture conditions. However, only ~56% and ~87% of DNA in dead sporozoites decayed by 3 and 6 h, respectively, and ~3.5% of the DNA remained in the culture for up to 16 h under the same conditions (Fig. 2B). These results suggest that DNA may remain in the culture for a longer period of time than RNA after the parasites are killed by drugs and strongly indicate that qRT-PCR is more likely to detect viable parasites than the qPCR assay. In other words, qPCR may overestimate the parasite level (and thus underestimate drug efficacy) if a compound under investigation kills cultured *Cryptosporidium* cells in the later stages of the parasite life cycle, because a significant amount of DNA from these dead parasites may persist for up to 16 h in the system.

Drug testing in vitro. We first validated the reliability of the qRT-PCR assay by examining the efficacies of NTZ and paromomycin in reducing the growth of two strains of *C. parvum* (IOWA and KSU-1) in vitro. NTZ is the only drug approved for use for the treatment of cryptosporidiosis, while paromomycin is a well established "gold standard" in drug testing

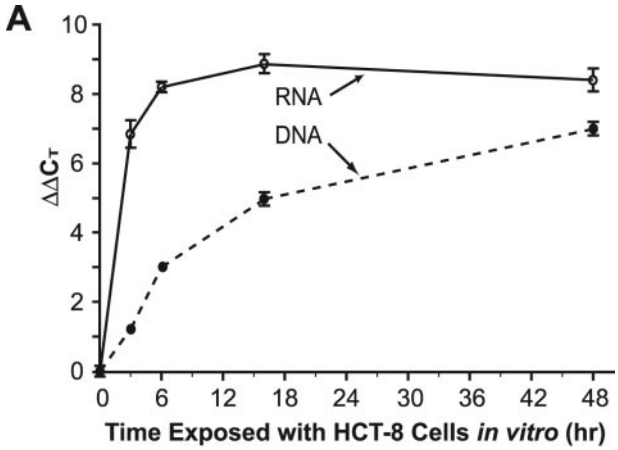

B

Time (hr)	0	3	6	16	48
DNA Decay (%)	0	56.2	87.0	96.5	99.1
RNA Decay (%)	0	98.9	99.6	99.8	99.7

FIG. 2. Decay of RNA and DNA in dead *C. parvum* sporozoites spiked into the HCT-8 cells in 24-well plates. After incubation at 37°C for the specified periods of time, total RNA and DNA were isolated for the detection of parasite and host cell 18S rRNA and the 18S rRNA gene by qRT-PCR and qPCR, respectively. The mean of the $\Delta\Delta C_T$ values at each time point of incubation was derived from at least two sample replicates, and each sample was subjected to at least two qRT-PCRs or qPCRs. (A) The $\Delta\Delta C_T$ values required for detection of parasite 18S rRNA (solid line) or the 18S rRNA gene (dashed line); (B) the percent decay of parasite RNA and DNA derived from the $\Delta\Delta C_T$ values by using the standard curves shown in Fig. 1. Bars represent standard errors of the means.

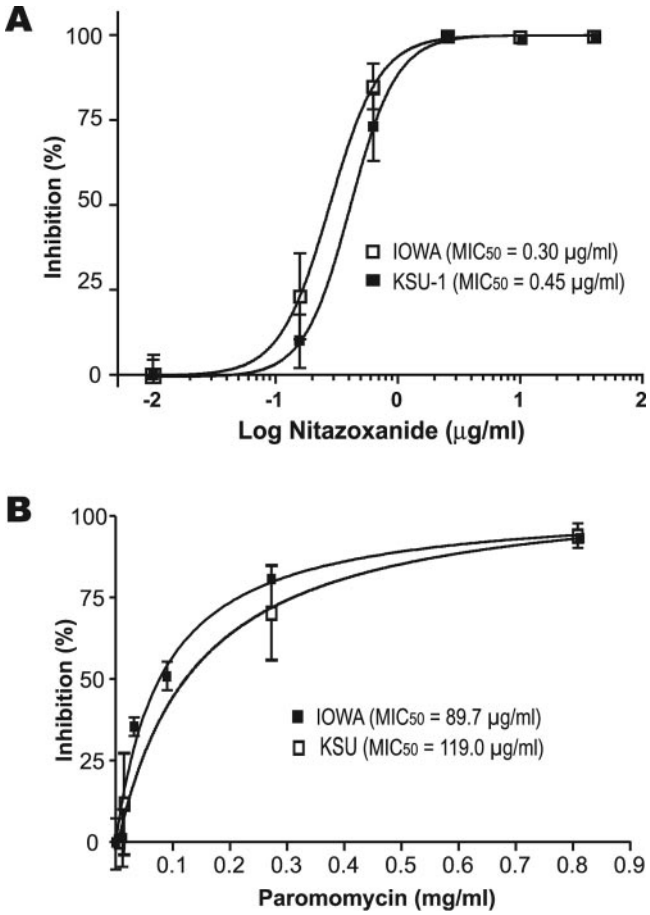

FIG. 3. Efficacies of nitazoxanide (A) and paromomycin (B) on the growth of *C. parvum* (IOWA and KSU-1 strains) in vitro, as determined by the qRT-PCR assay. The percent inhibition curves were derived by a nonlinear regression by using a hyperbolic equation (A) or sigmoidal model (B). Bars represent standard errors of the means derived from at least four replicates.

against *C. parvum* (11, 14, 18–20, 25, 28). In this test, both NTZ and paromomycin displayed dose-dependent inhibition of the IOWA and the KSU-1 strains of *C. parvum* cultured with HCT-8 cells (Fig. 3). The inhibition curves were well fit, as determined by nonlinear regressions. The MIC_{50} values for NTZ required to inhibit the IOWA and the KSU-1 strains were determined to be 0.30 and 0.45 μg/ml, respectively (Fig. 3A), which are slightly lower but comparable to the previously published value of 1.2 μg/ml (12). The growth of *C. parvum* in vitro was almost completely inhibited by NTZ at concentrations of 12.5 μg/ml or higher. The MIC_{50} values for paromomycin to inhibit the IOWA and the KSU-1 strains were determined to be 89.7 and 119.0 μg/ml, respectively, which is comparable to the published values determined by in situ enzyme-linked immunosorbent assay (25, 26), chemiluminescence immunoassay (28, 29), and microscopic methods (18). The maximum inhibition reached ~95% when paromomycin was used at a concentration of 810 μg/ml, which also agrees well with previously reported data.

Second, we employed the qRT-PCR assay to evaluate the efficacy of pyrazole on the growth of *C. parvum* in vitro. Pyrazole is an inhibitor of ADH (3, 7, 9, 17, 21). Recently, two distinct ADH genes (*CpADH1* and *CpADH-E*) have been discovered from the *C. parvum* and the *C. hominis* genomes (2). Therefore, testing of the efficacy of pyrazole has the potential for evaluation of whether these two ADH enzymes may be explored as novel drug targets against *Cryptosporidium* (2, 27). At concentrations ranging from 3.1 to 50 mM, pyrazole displayed a dose-dependent inhibition of the growth of *C. parvum* (IOWA strain) in vitro (R^2 = 0.9215) (Fig. 4A). The MIC_{50} determined by nonlinear curve regression was 15.8 mM, and a maximum inhibition of 93.4% was observed at a concentration of 50 mM. No significant cytotoxicity to HCT-8 cells was observed (by *t* test, $P = 0.001$) for pyrazole at any of the concentrations tested except the highest concentration (50 mM), in which a 28% reduction in enzyme activity was observed by the MTT (3-[4,5-dimethylthiazol-2-yl]-2,5-diphenyl tetrazolium bromide) assay (Fig. 4B). These observations suggest that pyrazole and analogs, as well as other ADH inhibitors, may be explored as potential drugs for the control of *C. parvum* infection.

DISCUSSION

We have established a qRT-PCR assay for the assessment of drug efficacy against *C. parvum* in vitro. By this method, the level of parasite 18S rRNA detected by qRT-PCR was used as an indicator of the parasite level in drug-treated samples. The

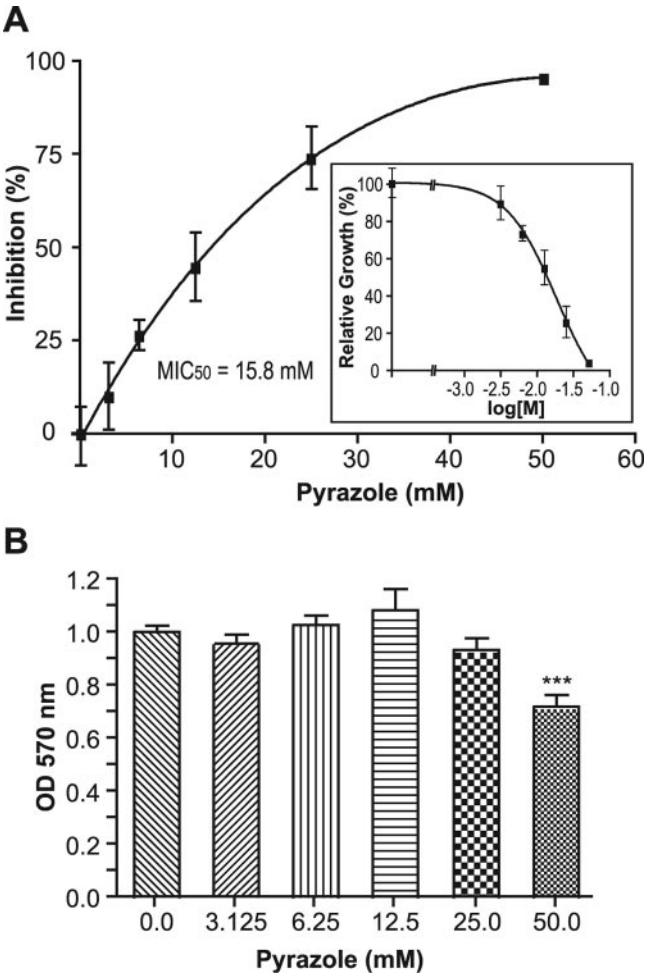

FIG. 4. Efficacy of pyrazole on the growth of *C. parvum* (IOWA strain) in vitro, as determined by the qRT-PCR assay. (A) Percent inhibition curve derived by a nonlinear regression by using a fourth-order polynomial equation. A similar curve was also obtained with a hyperbolic equation, albeit with a slightly higher variation (curve not shown). The inset shows the reversed sigmoidal curve representing the relative parasite growth against the logarithm of drug. (B) Cytotoxicity of pyrazole on HCT-8 cells, as determined by MTT assay. ***, value significantly different from that for the control (by *t* test, $P < 0.001$); OD, optical density. Bars represent standard errors of the means derived from at least four replicates.

level of parasite 18S rRNA was normalized by using that of the host cell 18S rRNA for each experimental condition. The reliability of the qRT-PCR assay was validated by testing the efficacies of NTZ and paromomycin as reference compounds. The observed MIC_{50} values for both compounds were comparable to the previously published ones.

Using the qRT-PCR assay, we also observed that pyrazole could inhibit the growth of *C. parvum* in vitro in a dose-dependent manner, which suggests that CpADH1 and CpADH-E may be explored as novel targets for drug development. However, our data on the efficacy of pyrazole is limited only to the in vitro model of *C. parvum* infection. Further studies with appropriate in vivo models of cryptosporidiosis are needed to confirm whether pyrazole and analogs may be truly developed into new anticryptosporidial drugs.

Because of the high sensitivity of the real-time PCR technology, it is critical to accurately add the same amount of RNA in all reactions. However, errors may easily be introduced in this step, either by pipetting errors during the manipulation of a large number of samples or because the RNA concentrations in the original samples cannot be accurately determined (e.g., contamination with minor amounts of protein, DNA, or other molecules is one of the possible common causes). The purpose of detecting the levels of both parasite and host cell 18S rRNA from the same samples and using host cell 18S rRNA as a reference control for normalization is to minimize these errors. In this study, the variations among plates and different experiments were greatly minimized in the qRT-PCR assay, as shown by both the SE of each experimental condition and the R^2 values (0.9893 and 0.9482 for the IOWA and the KSU-1 strains, respectively) of the standard curve (Fig. 1). Variations were higher when the thresholds for the detection of parasite 18S rRNA were not normalized by host 18S rRNA (data not shown), suggesting that the use of host RNA as a reference was a valid approach for the qRT-PCR (or qPCR, when applicable) detection of intracellular pathogens.

The present qRT-PCR assay is based on a SYBR green detection format, which is more economical than other detection methods and which can easily be adopted by other laboratories. However, it requires separate amplifications of parasite and host rRNA for each sample, and the normalization by using the host rRNA levels may not correct the potential pipetting errors introduced in this step (although it can be greatly minimized by careful operation). Therefore, there are potentials to further optimize the present qRT-PCR method by detecting both pathogen and host rRNA together in a single reaction by using a probe-based real-time RT-PCR, albeit with higher costs and the optimization of additional parameters.

The establishment of a qRT-PCR assay provides an alternative method to the currently available techniques for the evaluation of drug efficacy against *Cryptosporidium* in vitro. The algorithms provided and the concept of using the pathogen-to-host cell ratio for quantitative analysis may also be employed for screening for the effects of drug against other intracellular pathogens, including parasites, bacteria, and viruses. Because automated operation platforms are already available for cell culture, the isolation of nucleic acids, and the operation of PCR machines, this qRT-PCR method may potentially be adopted for high-throughput screening of the effects of drugs against *Cryptosporidium*.

ACKNOWLEDGMENTS

This study was funded in part by grants from the National Institute of Allergy and Infectious Diseases, National Institutes of Health (grants R21 AI055278 and R01 AI044594).

REFERENCES

1. **Abrahamsen, M. S., and A. A. Schroeder.** 1999. Characterization of intracellular *Cryptosporidium parvum* gene expression. Mol. Biochem. Parasitol. **104:**141–146.
2. **Abrahamsen, M. S., T. J. Templeton, S. Enomoto, J. E. Abrahante, G. Zhu, C. A. Lancto, M. Deng, C. Liu, G. Widmer, S. Tzipori, G. A. Buck, P. Xu, A. T. Bankier, P. H. Dear, B. A. Konfortov, H. F. Spriggs, L. Iyer, V. Anantharaman, L. Aravind, and V. Kapur.** 2004. Complete genome sequence of the apicomplexan, *Cryptosporidium parvum*. Science **304:**441–445.
3. **Andersson, P., J. Kvassman, A. Lindstrom, B. Olden, and G. Pettersson.** 1981. Effect of pH on pyrazole binding to liver alcohol dehydrogenase. Eur. J. Biochem. **114:**549–554.

4. **Cai, X., C. A. Lancto, M. S. Abrahamsen, and G. Zhu.** 2004. Intron-containing beta-tubulin transcripts in *Cryptosporidium parvum* cultured in vitro. Microbiology **150:**1191–1195.
5. **Chappell, C. L., and P. C. Okhuysen.** 2002. Cryptosporidiosis. Curr. Opin. Infect. Dis. **15:**523–527.
6. **Di Giovanni, G. D., and M. W. LeChevallier.** 2005. Quantitative-PCR assessment of *Cryptosporidium parvum* cell culture infection. Appl. Environ. Microbiol. **71:**1495–1500.
7. **Eklund, H., J. P. Samama, and L. Wallen.** 1982. Pyrazole binding in crystalline binary and ternary complexes with liver alcohol dehydrogenase. Biochemistry **21:**4858–4866.
8. **Fayer, R., U. Morgan, and S. J. Upton.** 2000. Epidemiology of *Cryptosporidium*: transmission, detection and identification. Int. J. Parasitol. **30:**1305–1322.
9. **Feierman, D. E., and A. I. Cederbaum.** 1987. Oxidation of the alcohol dehydrogenase inhibitor pyrazole to 4-hydroxypyrazole by microsomes. Effect of cytochrome P-450 inducing agents. Drug Metab. Dispos. **15:**634–639.
10. **Fox, L. M., and L. D. Saravolatz.** 2005. Nitazoxanide: a new thiazolide antiparasitic agent. Clin. Infect. Dis. **40:**1173–1180.
11. **Gargala, G., A. Delaunay, L. Favennec, P. Brasseur, and J. J. Ballet.** 1999. Enzyme immunoassay detection of *Cryptosporidium parvum* inhibition by sinefungin in sporozoite infected HCT-8 enterocytic cells. Int. J. Parasitol. **29:**703–709.
12. **Gargala, G., A. Delaunay, X. Li, P. Brasseur, L. Favennec, and J. J. Ballet.** 2000. Efficacy of nitazoxanide, tizoxanide and tizoxanide glucuronide against *Cryptosporidium parvum* development in sporozoite-infected HCT-8 enterocytic cells. J. Antimicrob. Chemother. **46:**57–60.
13. **MacDonald, L. M., K. Sargent, A. Armson, R. C. Thompson, and J. A. Reynoldson.** 2002. The development of a real-time quantitative-PCR method for characterisation of a *Cryptosporidium parvum* in vitro culturing system and assessment of drug efficacy. Mol. Biochem. Parasitol. **121:**279–282.
14. **Marshall, R. J., and T. P. Flanigan.** 1992. Paromomycin inhibits *Cryptosporidium* infection of a human enterocyte cell line. J. Infect. Dis. **165:**772–774.
15. **Morgan-Ryan, U. M., A. Fall, L. A. Ward, N. Hijjawi, I. Sulaiman, R. Fayer, R. C. Thompson, M. Olson, A. Lal, and L. Xiao.** 2002. *Cryptosporidium hominis* n. sp. (Apicomplexa: Cryptosporidiidae) from *Homo sapiens*. J. Eukaryot. Microbiol. **49:**433–440.
16. **Nesterenko, M. V., and S. J. Upton.** 1996. A rapid microcentrifuge procedure for purification of *Cryptosporidium* sporozoites. J. Microbiol. Methods **25:**87–89.
17. **Pereira, E. F., Y. Aracava, R. S. Aronstam, E. J. Barreiro, and E. X. Albuquerque.** 1992. Pyrazole, an alcohol dehydrogenase inhibitor, has dual effects on *N*-methyl-D-aspartate receptors of hippocampal pyramidal cells: agonist and noncompetitive antagonist. J. Pharmacol. Exp. Ther. **261:**331–340.
18. **Perkins, M. E., T. W. Wu, and S. M. Le Blancq.** 1998. Cyclosporin analogs inhibit in vitro growth of *Cryptosporidium parvum*. Antimicrob. Agents Chemother. **42:**843–848.
19. **Phelps, K. K., D. S. Lindsay, S. S. Sumner, and R. Fayer.** 2001. Immunohistochemistry based assay to determine the effects of treatments on *Cryptosporidium parvum* viability. J. Eukaryot. Microbiol. **48**(Suppl.)**:**40S–41S.
20. **Theodos, C. M., J. K. Griffiths, J. D'Onfro, A. Fairfield, and S. Tzipori.** 1998. Efficacy of nitazoxanide against *Cryptosporidium parvum* in cell culture and in animal models. Antimicrob. Agents Chemother. **42:**1959–1965.
21. **Trivic, S., and V. Leskovac.** 1994. Kinetic mechanism of yeast alcohol dehydrogenase activity with secondary alcohols and ketones. Indian J. Biochem. Biophys. **31:**387–391.
22. **Tzipori, S., and G. Widmer.** 2000. The biology of *Cryptosporidium*. Contrib. Microbiol. **6:**1–32.
23. **Upton, S. J., M. Tilley, and D. B. Brillhart.** 1995. Effects of select medium supplements on in vitro development of *Cryptosporidium parvum* in HCT-8 cells. J. Clin. Microbiol. **33:**371–375.
24. **Wilhelm, J., and A. Pingoud.** 2003. Real-time polymerase chain reaction. Chem. Biochem. **4:**1120–1128.
25. **Woods, K. M., M. V. Nesterenko, and S. J. Upton.** 1995. Development of a microtitre ELISA to quantify development of *Cryptosporidium parvum* in vitro. FEMS Microbiol. Lett. **128:**89–94.
26. **Woods, K. M., M. V. Nesterenko, and S. J. Upton.** 1996. Efficacy of 101 antimicrobials and other agents on the development of *Cryptosporidium parvum* in vitro. Ann. Trop. Med. Parasitol. **90:**603–615.
27. **Xu, P., G. Widmer, Y. Wang, L. S. Ozaki, J. M. Alves, M. G. Serrano, D. Puiu, P. Manque, D. Akiyoshi, A. J. Mackey, W. R. Pearson, P. H. Dear, A. T. Bankier, D. L. Peterson, M. S. Abrahamsen, V. Kapur, S. Tzipori, and G. A. Buck.** 2004. The genome of *Cryptosporidium hominis*. Nature **431:**1107–1112.
28. **You, X., M. J. Arrowood, M. Lejkowski, L. Xie, R. F. Schinazi, and J. R. Mead.** 1996. A chemiluminescence immunoassay for evaluation of *Cryptosporidium parvum* growth in vitro. FEMS Microbiol. Lett. **136:**251–256.
29. **You, X., M. J. Arrowood, M. Lejkowski, L. Xie, R. F. Schinazi, and J. R. Mead.** 1996. In vitro evaluation of anticryptosporidial agents using MDCK cell culture and chemiluminescence immunoassay. J. Eukaryot. Microbiol. **43:**87S.
30. **Zhu, G., and J. S. Keithly.** 1997. Molecular analysis of a P-type ATPase from *Cryptosporidium parvum*. Mol. Biochem. Parasitol. **90:**307–316.
31. **Zhu, G., J. S. Keithly, and H. Philippe.** 2000. What is the phylogenetic position of *Cryptosporidium*? Int. J. Syst. Evol. Microbiol. **50:**1673–1681.